Received April 20, 2021, accepted April 29, 2021, date of publication May 10, 2021, date of current version May 18, 2021.

Digital Object Identifier 10.1109/ACCESS.2021.3078454

Antenna Modeling Based on Two-Stage Gaussian Process Considering Sensitivity Information

RUI LI[1], YUBO TIAN[2], AND PENGFEI LI[1]
[1]School of Electronics and Information, Jiangsu University of Science and Technology, Zhenjiang 212003, China
[2]School of Information and Communication Engineering, Guangzhou Maritime University, Guangzhou 510725, China

Corresponding author: Yubo Tian (tianyubo@just.edu.cn)

This work was supported in part by the National Natural Science Foundation of China (NSFC) under Grant 61771225, and in part by the Qinglan Project of Jiangsu Higher Education.

ABSTRACT For antenna modeling and optimization design, high-fidelity full-wave electromagnetic simulation software can generally be used to obtain training samples. However, this process takes a long time. To solve this problem, a two-stage Gaussian process (GP) considering electromagnetic sensitivity information is proposed. Based on the coarse grid and fine grid of electromagnetic simulation software, the first stage learns the mapping relationships of antenna performance and sensitivity of each parameter, simultaneously. In the second stage, the accurate surrogates are established based on the mapping relationships above obtained. Because the method in this study takes sensitivity information into consideration during the modeling process, it can better reflect the mapping relationship between antenna input and output, which can develop a more accurate surrogate model. The proposed two-stage GP surrogate model considering sensitivity information can significantly reduce the demand of high-fidelity training samples for modeling, and greatly save the simulation time of calling electromagnetic simulation software. Therefore, this method is more suitable for the problems of insufficient electromagnetic simulation samples. The proposed approach is evaluated by modeling and optimization of an inverted F antenna and an ultra-wideband planar monopole antenna. The results show that the method has high modeling accuracy with limited training samples given by high-fidelity electromagnetic simulation, which further verify its effectiveness and efficiency.

INDEX TERMS Gaussian process, sensitivity information, electromagnetic optimization, antenna.

I. INTRODUCTION

With the rapid development of computer field, computer aided design (CAD) technology has been greatly improved, and it is also used for simulation design of electromagnetic problems [1], generally using full-wave electromagnetic simulation software including high frequency structural simulator (HFSS), Computer Simulation Technology (CST), etc. When optimizing the electromagnetic problems, global optimization algorithms, such as particle swarm optimization (PSO) [2]–[5], genetic algorithm (GA) [6]–[8] ant colony optimization (ACO) [9]–[11] etc., are usually used in combination with electromagnetic simulation software. However, this process repeatedly calls electromagnetic simulation software for electromagnetic performance evaluation, which is very time-consuming. Therefore, how to reduce the calculation time and quickly optimize complex problem is crucial. Two kinds of optimization methods to solve this problem include performance driven optimization and EM-based stochastic optimization. Performance-driven optimization may need to deal with a considerable range of antenna parameters [12], [13]. Reference [14] employs the overall performance-driven modeling to construct a fast surrogate in the region corresponding to maximum changes of the antenna response in the vicinity of the nominal design to solve the problem of multi-band antenna yield optimization. The EM-based stochastic optimization method involves surrogate models in actual problems, and the process of establishing these models is relatively simple and stable, which can replace the electromagnetic simulation software to perform a limited number of real function evaluation. For the modeling and optimization of the antenna in this paper, the latter is more applicable. Among them, surrogate models are usually used, including artificial neural network (ANN) [15]–[17], support vector machine (SVM) [18]–[20] and Gaussian process (GP) [21]–[23] and so on.

The associate editor coordinating the review of this manuscript and approving it for publication was Ting Wang.

TABLE 1. Electromagnetic application.

AI-based approach	Antenna type	Dimension(mm^2)	-10dB Band (GHz)	Gain(dB)
PSO	UWB[4]	32×28	3.1-10.6GHz	2dB at 7GHz
	Fractal antenna[5]	31.8×24	5.2-6.4GHz	4.6dB at 5.8GHz
	PIFA[6]	41×40	3.38-4.45GHz	3.35dB at 3.5GHz
GA	PIFA[6]	41×40	3.324-4.002GHz	2.58dB at 3.5GHz
	UWB[7]	34.45×23.85	3.1-12GHz	6.46dB at 12GHz
	Elliptical UWB antenna[8]	33×30	3.1-10.6GHz	2.4dB at 7GHz
ACO	E-shaped wideband patch antenna[10]	42.36×21.59	4.8-6.53GHz	10dB at 5.5GHz
	Compact broadband CP slot antenna[11]	20×40	3.7-11.1GHz	8dB at 8.6GHz
ANN	Single band-notch UWB antenna[15]	36×24	2.8-5.3GHz 6.0-8.5GHz	2.77dB at 3.3GHz 5.70dB at 6.6GHz
	Dual Ring Antenna[16]	40×40	2.41-2.5GHz	4dB at 2.45GHz
SVM	Rectangular microstrip antenna[19]	7×7	2.13-2.19GHz	7.02dB at 2.15GHz
GP	PIFA[22]	120×60	0.88-0.98GHz	3.45dB at 0.92GHz
	Yagi MSA[23]	120×60	2.2-2.4GHz	7.4dB at 2.3GHz

The artificial intelligence-based algorithms commonly applied in the antenna design in recent years, are shown in Table 1. The popular ANN not only needs a large number of labeled samples, but also has no standard structure framework. The kernel function parameters of SVM are difficult to determine, which is easy to produce over fitting problems. In contrast, GP has a strict statistical theoretical basis, which is suitable for dealing with small samples, high dimensions, nonlinear and other complex problems [24]. The strong modeling capabilities of GP make it possible to adaptively obtain hyper-parameters and realize probabilistic prediction that is different from other regression models, so it is more and more widely used in the analysis of antenna modeling problems [25]–[29].

When electromagnetic performance is evaluated and calculated by electromagnetic simulation software, if HFSS or CST software is used, the simulation results not only include conventional electromagnetic performance, but also provide sensitivity information [30]–[33]. Sensitivity information is defined as the ratio of electromagnetic response or changes of solution results to design geometric parameters. In [34], the sensitivity derivative information is successfully combined with multi-layer perception neural network to successfully model and design the radar cross section (RCS) of the nonlinear loaded antenna; similarly, the sensitivity information combined with space mapping technology can effectively model microwave and RF components [35]. Then, a new adjoint neural network technology based on sensitivity analysis was proposed in [30], and the parametric model of microwave passive components was successfully established. This technology can not only learn the mapping relationship between the input and output of the modeling problem, but also learn the electromagnetic sensitivity information, and develop the parameter model with high robustness. In recent years, most of the alternative models combined with sensitivity information are neural networks. In this paper, we expand the modeling method that considers sensitivity information, and propose a GP modeling method that considers sensitivity information. Because a certain number of high-precision training samples are needed in the modeling process of GP, the calculation burden of sample acquisition is large. To a certain extent, it can be solved by two-stage Gaussian process [36]. Based on this, the sensitivity information will be introduced into the modeling process, and the change trend of electromagnetic response can be obtained at the same time. The advantage is that it can develop a more accurate surrogate model. Moreover, in HFSS or CST, the simulation time of sensitivity information is relatively short and can be obtained simultaneously with the electromagnetic response performance, without too much additional simulation time. In this study, the two-stage antenna performance GP and sensitivity GP are established simultaneously. Their input parameters are the same, and their outputs are electromagnetic response and sensitivity information respectively. Therefore, the proposed model can obtain the electromagnetic performance response of input parameters and sensitivity information of each parameter at the same time. The modeling method has two stages. The first stage uses HFSS with coarse grids to generate n low-fidelity performance training samples and corresponding n low-fidelity sensitivity training samples, from which n_{fine} ($n_{\text{fine}} < n$) samples are selected to generate high-fidelity performance samples and high-fidelity sensitivity samples

based on HFSS with fine grids. Two GPs are used to simultaneously learn the mapping relationship between the coarse and the fine model of antenna performance and sensitivity information, predicting $(n - n_{\text{fine}})$ high-fidelity performance outputs and sensitivity outputs corresponding to low-fidelity. The second stage combines n_{fine} high-fidelity outputs simulated by HFSS and $(n-n_{\text{fine}})$ predicted outputs by the trained GPs in the first stage to establish antenna performance GP and sensitivity GP. The training errors sum of the two GPs is minimized, and then a surrogate model with higher accuracy is established to obtain accurate antenna performance output. Two different antennas, including an inverted F antenna and an ultra-wideband planar monopole antenna, are used to evaluate the effectiveness of the proposed method.

II. THE PROPOSED SURROGATE MODEL CONSIDERING SENSITIVITY INFORMATION

A. BASIC PRINCIPLES OF SENSITIVITY

Sensitivity is defined as the ratio of electromagnetic response or solution results to the changes of design geometric parameters or material parameters. Take S_{11} as an example, assuming $x_{\text{i}}\,(i = 1, 2, \ldots, m)$ is a set geometric parameter, the sensitivity of the transmission coefficient $S_{\text{jk}}\,(i = 1, 2, \ldots, n)$ between k and j ports to the design parameter is defined as

$$\mathrm{C}_{x_{\text{i}}}^{S_{\text{jk}}} = \frac{\partial S_{\text{jk}}}{\partial x_{\text{i}}} \tag{1}$$

Sensitivity equation (1) can quantify the influence of various parameters on electromagnetic characteristic, and considering the sensitivity information when modeling can improve the accuracy of the surrogate.

B. GAUSSIAN PROCESS

Gaussian process (GP) is a Bayesian nonparametric regression technique, and its properties are determined by the mean function and the covariance function [37], which are defined by

$$\begin{cases} m\left(\boldsymbol{x}\right) = E\left[f\left(\boldsymbol{x}\right)\right] \\ k\left(\boldsymbol{x}, \boldsymbol{x}'\right) = E\{[(\boldsymbol{x}) - m\left(\boldsymbol{x}\right)]\left[f\left(\boldsymbol{x}'\right) - f\left(\boldsymbol{x}'\right)\right]\} \end{cases} \tag{2}$$

where $\boldsymbol{x}, \boldsymbol{x}' \in R^{\text{d}}$, $m(\boldsymbol{x})$ and $k(\boldsymbol{x}, \boldsymbol{x}')$ are the mean function and covariance function.

Assuming the model $y = f(\text{x}) + \varepsilon$, the observed target value y contaminated by additive noise ε, which is a random variable that obeys the normal distribution

$$\varepsilon \sim N(0, \sigma_n^2) \tag{3}$$

then the prior distribution of y is given by

$$y \sim N(0, \boldsymbol{K} + \sigma_n^2 \boldsymbol{I}) \tag{4}$$

where $\boldsymbol{K} = K(X, X)$ is a symmetric positive definite covariance matrix of order $n \times n$, k_{ij} measures the correlation between $\boldsymbol{x}_{\text{i}}$ and $\boldsymbol{x}_{\text{j}}$. The jointly Gaussian prior distribution of n training sample outputs y and n^* test sample outputs f^* is calculated by

$$\begin{bmatrix} y \\ f* \end{bmatrix} \sim N\left(0, \begin{pmatrix} K(X,X) + \sigma_n^2 \boldsymbol{I} & K(X, X*) \\ K(X*, X) & K(X*, X*) \end{pmatrix}\right) \tag{5}$$

GP can choose different covariance functions [38], which usually use the square exponential function

$$k(\boldsymbol{x}, \boldsymbol{x}') = \sigma_f^2 exp[-0.5(\boldsymbol{x} - \boldsymbol{x}')^T M(\boldsymbol{x} - \boldsymbol{x}')] \tag{6}$$

The properties of the mean function and covariance function of GP are determined by a set of hyper parameters, and the maximum likelihood function can be used to find the optimal hyper parameters. By establishing the log likelihood function of the conditional probability of the training samples, the partial derivative of the hyper parameter is obtained, and then the conjugate gradient optimization method is used to find the optimal solution of the hyper parameter. The form of the negative log likelihood function is given by

$$\boldsymbol{I} = logp(y|X) = -\frac{1}{2} y^T K^{-1} y - \frac{1}{2} log|K| - \frac{n}{2} log 2\pi \tag{7}$$

Given new input $\overset{*}{x}$, the input value $\boldsymbol{x}$ of the training set, and the observed target value y, the maximum possible prediction posterior distribution of $\overset{*}{y}$ is inferred as

$$p(y^*|x^*, \boldsymbol{X}, \boldsymbol{y}) = N(\boldsymbol{m}, \boldsymbol{\Sigma}) \tag{8}$$

where the predicted mean $\boldsymbol{m}$ and covariance $\boldsymbol{\Sigma}$ are given by

$$\boldsymbol{m} = \boldsymbol{K}(\boldsymbol{X}^*, \boldsymbol{X})\boldsymbol{K}(\boldsymbol{X}, \boldsymbol{X})^{-1}\boldsymbol{y} \tag{9}$$

$$\boldsymbol{\Sigma} = \boldsymbol{K}(\boldsymbol{X}^*, \boldsymbol{X}^*) - \boldsymbol{K}(\boldsymbol{X}^*, \boldsymbol{X})\boldsymbol{K}(\boldsymbol{X}, \boldsymbol{X})^{-1}\boldsymbol{K}(\boldsymbol{X}, \boldsymbol{X}^*) \tag{10}$$

The prediction mean and variance of GP model describe a Gaussian distribution that the prediction output may obey. If the prediction mean is regarded as the prediction output value of general nonlinear fitting tools, the prediction variance can actually be regarded as the evaluation of the uncertainty of the prediction mean, and its value reflects the accuracy of GP model at this point.

C. MODELING PROCESS CONSIDERING SENSITIVITY INFORMATION

In order to solve the problem that GP requires a large number of high-fidelity training data samples and high computational cost, a two-stage GP antenna modeling method considering sensitivity information is adopted.

1) FIRST STAGE

Performance simulation and sensitivity simulation of n groups of size parameters are carried out with h frequency points uniformly selected for each group of size based on HFSS with coarse grid, obtaining n groups of low-fidelity electromagnetic performance training set $\boldsymbol{D}_{\text{coar,perf}}$ and sensitivity information training set $\boldsymbol{D}_{\text{coar,sens}}$:

$$\boldsymbol{D}_{\text{coar,perf}} = \left\{\left(\boldsymbol{u}_i, \boldsymbol{y}_{\text{coar,perf},i}\right)|i = 1, \cdots, n\right\} \tag{11}$$

$$\boldsymbol{D}_{\text{coar,sens}} = \left\{\left(\boldsymbol{u}_i, \boldsymbol{y}_{\text{coar,sens},i}\right)|i = 1, \cdots, n\right\} \tag{12}$$

$$\boldsymbol{u}_i = [\boldsymbol{X}_i, f_{ih}] = [x_{1i}, x_{2i}, \cdots, x_{Pi}, f_{ih}] \quad (13)$$

where $\boldsymbol{u}_i$ is the ith training input vector, which includes the P-dimensional antenna geometric parameter $[\mathrm{x}_{1i}, \mathrm{x}_{2i}, \cdots, \mathrm{x}_{Pi}]$ and h antenna frequencies f_{ih}; $\boldsymbol{y}_{\mathrm{coar,perf},\,i}$ and $\boldsymbol{y}_{\mathrm{coar,sens},\,i}$ respectively represent ith low-fidelity electromagnetic performance response and sensitivity information of the HFSS with coarse grid. Randomly select $n_{\mathrm{fine}}(n_{\mathrm{fine}} < n)$ groups from n groups of low-fidelity electromagnetic performance data sets and sensitivity information data sets, and simulate the corresponding high-fidelity electromagnetic performance $\boldsymbol{D}_{\mathrm{fine,perf}}$ and high-fidelity sensitivity information $\boldsymbol{D}_{\mathrm{fine,sens}}$ based on the HFSS fine grid as follows:

$$\boldsymbol{D}_{\mathrm{fine,perf}} = \left\{\left(\boldsymbol{u}_{\mathrm{perf},j}, \boldsymbol{y}_{\mathrm{fine,perf},\,j}\right) | j = 1, \cdots, n_{\mathrm{fine}}\right\} \quad (14)$$

$$\boldsymbol{D}_{\mathrm{fine,sens}} = \left\{\left(\boldsymbol{u}_{\mathrm{sens},j}, \boldsymbol{y}_{\mathrm{fine,sens},\,j}\right) | j = 1, \cdots, n_{\mathrm{fine}}\right\} \quad (15)$$

$$\boldsymbol{u}_{\mathrm{perf},\,j} = \left[x_{1j}, x_{2j}, \cdots, x_{Pj}, f_{jh}, \boldsymbol{y}_{\mathrm{coar,perf},\,j}\right]^{\mathrm{T}} \quad (16)$$

$$\boldsymbol{u}_{\mathrm{sens},\,j} = \left[x_{1j}, x_{2j}, \cdots, x_{Pj}, f_{jh}, \boldsymbol{y}_{\mathrm{coar,sens},\,j}\right]^{\mathrm{T}} \quad (17)$$

where $\boldsymbol{u}_{\mathrm{perf},j}$ and $\boldsymbol{u}_{\mathrm{sens},j}$ respectively represent jth training input vector composed of antenna geometric size, antenna frequency with low-fidelity electromagnetic performance response and sensitivity information. Then using input data $\boldsymbol{u}_{\mathrm{perf},j}$ and output data $\boldsymbol{y}_{\mathrm{fine,perf},j}$ establish a GP, which reflects the mapping relationship between the coarse and fine grids. The trained GP is used to predict the remaining $(n - n_{\mathrm{fine}})$ groups of electromagnetic performance response values $\boldsymbol{y}_{\mathrm{pred,perf},j} | j = 1, 2, \cdots, n - n_{\mathrm{fine}}$. By the same way, the $(n - n_{\mathrm{fine}})$ groups of sensitivity information $\boldsymbol{y}_{\mathrm{pred,sens},j}$ are predicted. Finally, the training set $\boldsymbol{D}_{\mathrm{fine,perf,appr}}$ composing by the n_{fine} high-fidelity electromagnetic performance response and the $(n - n_{\mathrm{fine}})$ prediction values is given by (18). Similarly, the joint sensitivity information training set $\boldsymbol{D}_{\mathrm{fine,sens,appr}}$ is given by (19).

$$\boldsymbol{D}_{\mathrm{fine,perf,appr}} = \left\{ \begin{array}{c} (\boldsymbol{u}_k, \boldsymbol{y}_{\mathrm{fine,perf},k}) | k = 1, \cdots, n_{\mathrm{fine}} \\ (\boldsymbol{u}_k, \boldsymbol{y}_{\mathrm{pred,perf},k}) | k = (n_{\mathrm{fine}} + 1), \cdots, n \end{array} \right\} \quad (18)$$

$$\boldsymbol{D}_{\mathrm{fine,sens,appr}} = \left\{ \begin{array}{c} (\boldsymbol{u}_k, \boldsymbol{y}_{\mathrm{fine,sens},k}) | k = 1, \cdots, n_{\mathrm{fine}} \\ (\boldsymbol{u}_k, \boldsymbol{y}_{\mathrm{pred,sens},k}) | k = (n_{\mathrm{fine}} + 1), \cdots, n \end{array} \right\} \quad (19)$$

2) SECOND STAGE

Here we use $\boldsymbol{D}_{\mathrm{fine,perf,appr}}$ and $\boldsymbol{D}_{\mathrm{fine,sens,appr}}$ to establish antenna performance GP and sensitivity GP. Exploiting the prediction results of the GPs established in the first stage, the accuracy of final surrogate model will almost not be affected even if the amount of high-fidelity training data is reduced in the second stage, saving a lot of time for getting more high-fidelity training samples. When training the GPs, we consider not only the performance error but also the sensitivity error. As a high efficient global optimization algorithm, PSO is used to minimize the total training error E_T given by

$$\begin{aligned} E_T &= E_{pe} + E_{se} \\ &= \sum_{i \in Q} (\boldsymbol{y}_{\mathrm{pred,perf},i} - \boldsymbol{y}_{\mathrm{hfss,perf},i})^2 \\ &\quad + A \sum_{p \in P, i \in Q} (\boldsymbol{y}_{\mathrm{pred,sens},i,p} - \boldsymbol{y}_{\mathrm{hfss,sens},i,p})^2 \end{aligned} \quad (20)$$

$$\boldsymbol{y}_{\mathrm{pred,sens},i,p} = \frac{\partial \boldsymbol{y}_{\mathrm{pred,sens},i}}{\partial x_p} \quad (21)$$

$$\boldsymbol{y}_{\mathrm{hfss,sens},i,p} = \frac{\partial \boldsymbol{y}_{\mathrm{hfss,sens},i}}{\partial x_p} \quad (22)$$

where E_{pe} and E_{se} respectively represent the training errors of the antenna performance GP and the sensitivity GP; $\boldsymbol{y}_{\mathrm{pred,perf},i}$ and $\boldsymbol{y}_{\mathrm{hfss,perf},i}$ respectively represent the predicted output of the ith group of geometric parameters of the antenna performance GP and the simulation response of HFSS; x_p represents the pth element of the input vector $\boldsymbol{x}$; $\boldsymbol{y}_{\mathrm{pred,sens},i,p}$ and $\boldsymbol{y}_{\mathrm{hfss,sens},i,p}$ respectively represent the predicted output derivatives and the simulation output derivatives by HFSS of the pth input element; P and Q respectively represent the geometric parameter dimension and the number of output samples; A represents the weight coefficient of the sensitivity error function. Finally, the established surrogate model is used as the fitness function of the particle swarm optimization (PSO) to optimize the antenna size. Specially, in this paper, the acceleration coefficients are 2, and the inertia weight decreases linearly from 1 to 0, and the swarm size is 50.

The overall design steps of the proposed method are summarized as follows.

1) Use partial combination orthogonal experimental design to select n groups antenna sizes, establish a MATLAB-HFSS simulation model, and obtain n groups low-fidelity electromagnetic performance response and sensitivity information with h frequency points based on HFSS with coarse grid.
2) Select $n_{\mathrm{fine}}(n_{\mathrm{fine}} < n)$ groups antenna from the n groups, and compute n_{fine} groups high-fidelity electromagnetic performance response and sensitivity information based on HFSS with fine grid. Combining the low-fidelity performance response and sensitivity information of step 1), the performance GP_1 and sensitivity GP_3 are established from the obtained data with coarse and fine grids. The remaining $(n - n_{\mathrm{fine}})$ groups of the low-fidelity performance response and sensitivity information are taken as the input of GP_1 and GP_3, and the corresponding 'precise' electromagnetic performance response and 'precise' sensitivity information are predicted respectively.
3) Combining n_{fine} groups high-fidelity performance data and $(n - n_{\mathrm{fine}})$ groups predicted 'precise' data by GP_1 establish antenna performance GP_2. simultaneously, combining n_{fine} groups high-fidelity sensitivity information and $(n - n_{\mathrm{fine}})$ groups predicted 'precise' data by GP_3 establish sensitivity GP_4.
4) The two-stage GP with sensitivity information is trained to minimize E_T.
5) Initialize the population and parameters of the PSO.
6) The fitness function is constructed by the trained GP_2 and GP_4 in the light of (20), (21), (22).

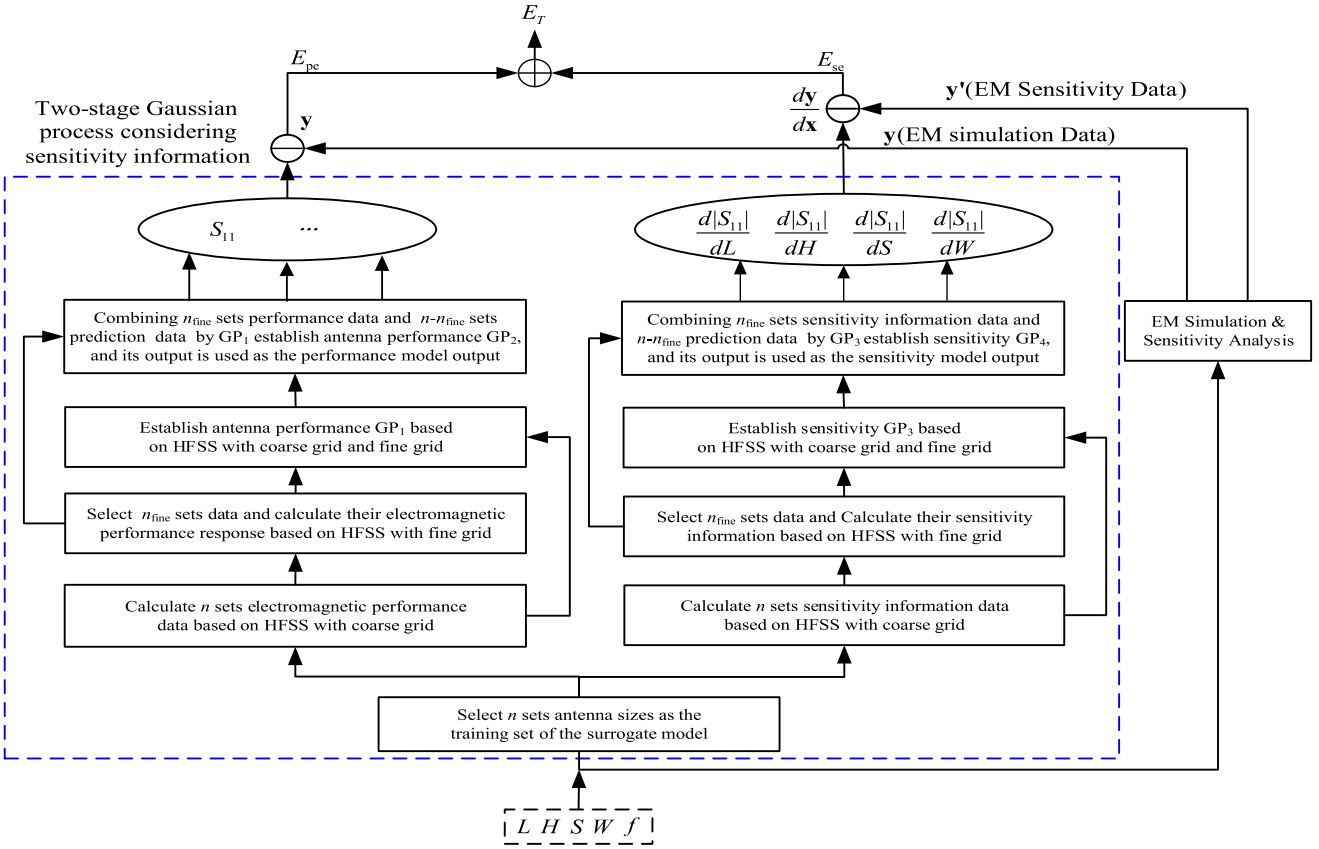

(a). Two-stage Gaussian process modeling considering sensitivity information

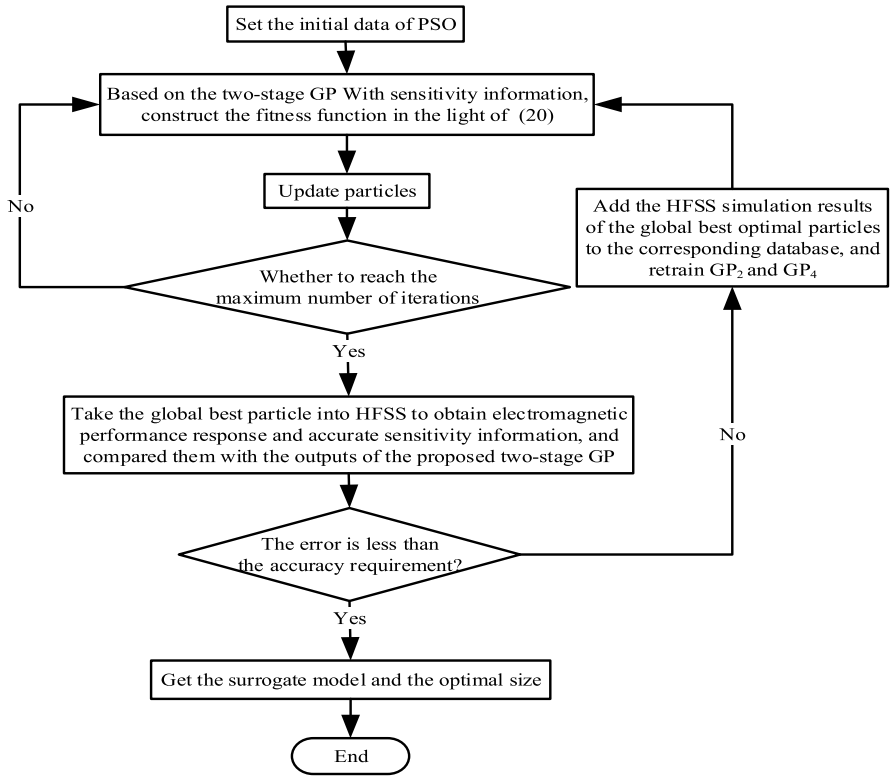

(b). Optimization by the trained surrogate model combined with PSO algorithm

FIGURE 1. Flowchart of the proposed method.

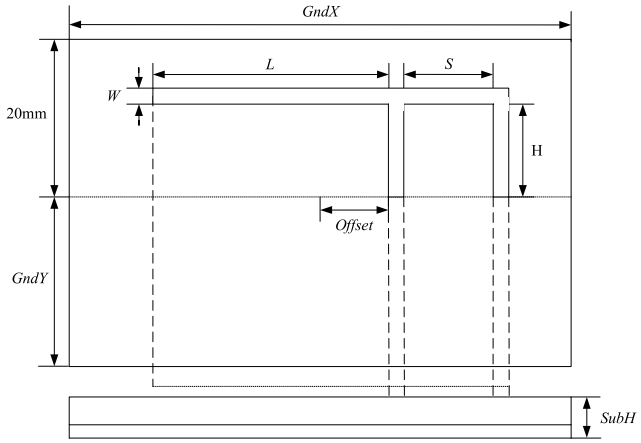

(a). structure model

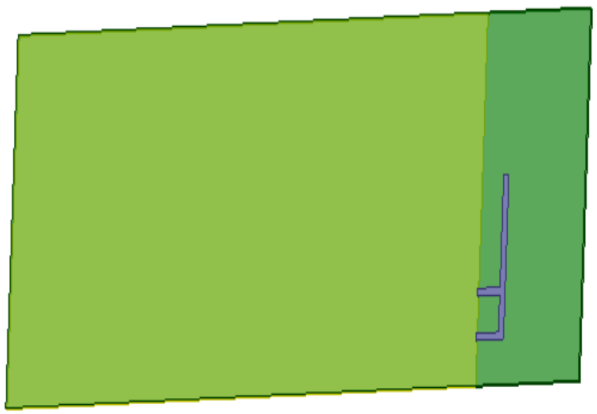

(b). HFSS model

FIGURE 2. The inverted F antenna.

7) The iteration for the optimization is carried out. If reaching the maximum number of iterations, it will jump out of the loop and output the global best particle and optimal fitness value. If not, it will return and continue the loop.
8) Simulate the global best particle by HFSS to obtain high-fidelity electromagnetic performance response and sensitivity information, and compare them with the outputs of the proposed two-stage GP considering sensitivity information. If the error is greater than the threshold, we will update the model; if not, we will output the result and get the antenna parameters that meet the optimization conditions.

Figure 1 is the flowchart of the proposed method, in which L, H, S, and W are geometric parameters of the optimized antenna, and f is the frequency. There are two parts in Figure 1, among which Figure 1(a) is modeling flowchart of the two-stage GP based on sensitivity, which contains antenna performance response and sensitivity information, and Figure 1(b) is optimization flowchart of the trained surrogate model in Figure 1(a) combined with PSO algorithm.

III. PERFORMANCE TEST AND EVALUTION

In this section, we will use the proposed two-stage GP considering sensitivity information to model and optimize the inverted F antenna in [39] and the ultra-wideband planar monopole antenna in [40].

A. THE INVERTED F ANTENNA

The structure model of the inverted F antenna in [39] is shown in Figure 2(a), and its HFSS model is shown in Figure 2(b), which includes inverted F-shaped antenna, substrate layer and ground plate. The frequency band of interest is 1.8GHz∼3.2GHz. The electromagnetic performance of the antenna is mainly determined by length L, height H, distance S between ground point and feed point, and width W of microstrip line. The design ranges are L=[15.5,17]mm, H=[2.8,4.3]mm, S=[3,7]mm, and W=[0.8,1.2]mm, respectively. Among them, the upper and lower limit width of the design variables are determined according to the empirical values of [39]. Other fixed geometric parameters of the antenna are shown in Table 2. The optimization indexes are that S_{11} at resonance frequency is less than -20dB, and bandwidth at -10dB is greater than 100MHz.

Setting the iteration number of HFSS with coarse grid is 3, fine grid is 7, precision is 0.02, and sensitivity variables are L, H, S and W. In the first stage, number of training samples is 50, with 50 frequency points for one sample, and the training input is $\{\boldsymbol{u}_i = [\boldsymbol{X}_i, f_{ih}] = [L_i, H_i, S_i, W_i, f_{ih}] | i = 1, 2, \cdots, n\}$. According to n ($n = 50$) groups of antennas selected in the experiment, we can obtain $\boldsymbol{y}_{\text{coar,perf},i}$ and $\boldsymbol{y}_{\text{coar,sens},i}$, namely $|S_{11}|_{coar}$, and $\frac{d|S_{11}|}{dL}_{\text{coar}}$, $\frac{d|S_{11}|}{dH}_{\text{coar}}$, $\frac{d|S_{11}|}{dS}_{\text{coar}}$, $\frac{d|S_{11}|}{dW}_{\text{coar}}$ by HFSS with coarse grid to form $\boldsymbol{D}_{\text{coar,perf}}$ and $\boldsymbol{D}_{\text{coar,sens}}$. 20 groups are randomly selected from the 50 samples, and we use HFSS with fine grid to simulate their $\boldsymbol{y}_{\text{fine,perf},i}$ and $\boldsymbol{y}_{\text{fine,sens},i}$, namely $|S_{11}|_{fine}$, and $\frac{d|S_{11}|}{dL}_{\text{fine}}$, $\frac{d|S_{11}|}{dH}_{\text{fine}}$, $\frac{d|S_{11}|}{dS}_{\text{fine}}$, $\frac{d|S_{11}|}{dW}_{\text{fine}}$ to form $\boldsymbol{D}_{\text{fine,perf}}$ and $\boldsymbol{D}_{\text{fine,sens}}$. According to the 20 groups of samples given by HFSS with coarse and fine grid, the antenna performance GP_1 and sensitivity GP_3 are established, and then use them to predict the remaining 30 groups of $\boldsymbol{y}_{\text{pred,perf},j}$ and $\boldsymbol{y}_{\text{pred,sens},j}$, namely $|S_{11}|_{pred}$, and $\frac{d|S_{11}|}{dL}_{\text{pred}}$, $\frac{d|S_{11}|}{dH}_{\text{pred}}$, $\frac{d|S_{11}|}{dS}_{\text{pred}}$, $\frac{d|S_{11}|}{dW}_{\text{pred}}$. Finally, we combine the 20 groups high-fidelity simulation samples given by HFSS and the 30 groups predicted 'precise' samples given by the trained GP_1 and GP_3 to form new training samples, namely $\boldsymbol{D}_{\text{fine,perf,appr}}$ and $\boldsymbol{D}_{\text{fine,sens,appr}}$, and then use them to train antenna performance surrogate model GP_2 and sensitivity surrogate model GP_4.

The definition of the training samples and test samples of the inverted F antenna is shown in Table 3, and the test results of the trained two-stage GP considering the sensitivity information model are shown in Table 4. The average absolute

TABLE 2. Fixed structure parameters of the inverted F antenna.

Structure name	variable name	Variable value (unit: mm)
Thickness of substrate layer	*SubH*	0.8
Length of grounding plate	*GndY*	90
Width of grounding plate	*GndX*	50
Transverse distance from feed point to coordinate origin	*Offset*	12
Wavelength of free space	*Lambda*	122.4

TABLE 3. Training and test samples for the inverted F antenna.

Parameters (Sensitivity Variables)	Training data			Testing data		
	Min	Max	Step	Min	Max	Step
L(mm)	15.5	17	0.5	15.3	16.8	0.5
H(mm)	2.8	4.3	0.5	3	4.5	0.5
S(mm)	4	7	1	3.5	6.5	1
W(mm)	0.9	1.2	0.1	0.85	1.15	0.1

TABLE 4. Errors of different test samples for the inverted F antenna.

No.	1	2	3	4	5
MAE(dB)	0.4703	0.4876	0.3417	0.4273	0.6061
RMSE(dB)	0.7243	0.6151	0.4803	0.6044	0.8859

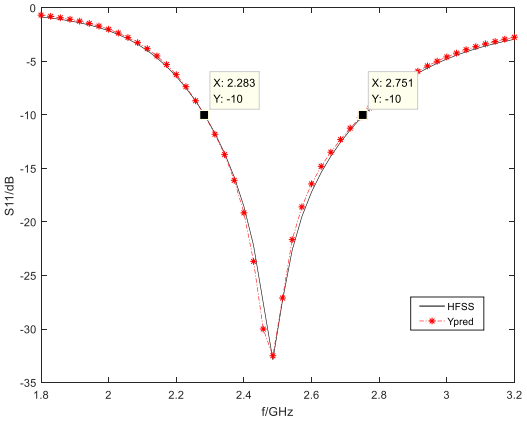

FIGURE 3. S_{11} of the optimized inverted F antenna.

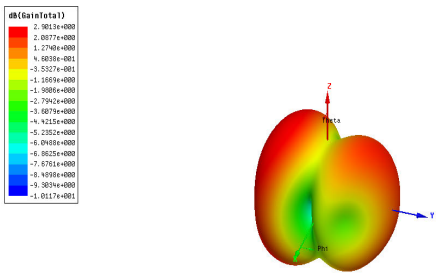

FIGURE 4. Three-dimensional gain pattern of the optimized inverted F antenna.

error (MAE) and root mean squared error (RMSE) are used to evaluate the performance of the trained model, and they are formulated by

$$\mathrm{MAE} = \frac{1}{h}\sum_{i=1}^{h}|\boldsymbol{y}_{\mathrm{pred},i} - \boldsymbol{y}_i| \tag{23}$$

$$\mathrm{RMSE} = \sqrt{\frac{1}{h}\sum_{i=1}^{h}(\boldsymbol{y}_{\mathrm{pred},i} - \boldsymbol{y}_i)^2} \tag{24}$$

where $\boldsymbol{y}_{\mathrm{pred},i}$ and $\boldsymbol{y}_i$ are the predicted values at the ith frequency point of the trained two-stage GP model considering sensitivity information and its high-fidelity HFSS simulation result, respectively. It can be seen from Table 4 that the MAE is about 0.5, RMSE is about 0.6, and they are all small, which verifies the effectiveness of the proposed modeling method.

Taking the trained model as fitness function, we use PSO to optimize the antenna, and the result is [15.9963 3.7660 4.8463 1.0148] mm, its S_{11} is shown in Figure 3, where the black solid represents the simulation result by electromagnetic simulation software HFSS, and the red dash line with star represents the predicted result by the proposed algorithm. It can be seen from Figure 3 that the value of S_{11} at the resonance frequency point is less than -20dB, and the bandwidth at -10dB is significantly greater than 100MHz, which meets the design requirements. Compared with the simulation results of electromagnetic simulation software, the prediction error at the resonance point is also relatively small, and the electromagnetic simulation and the

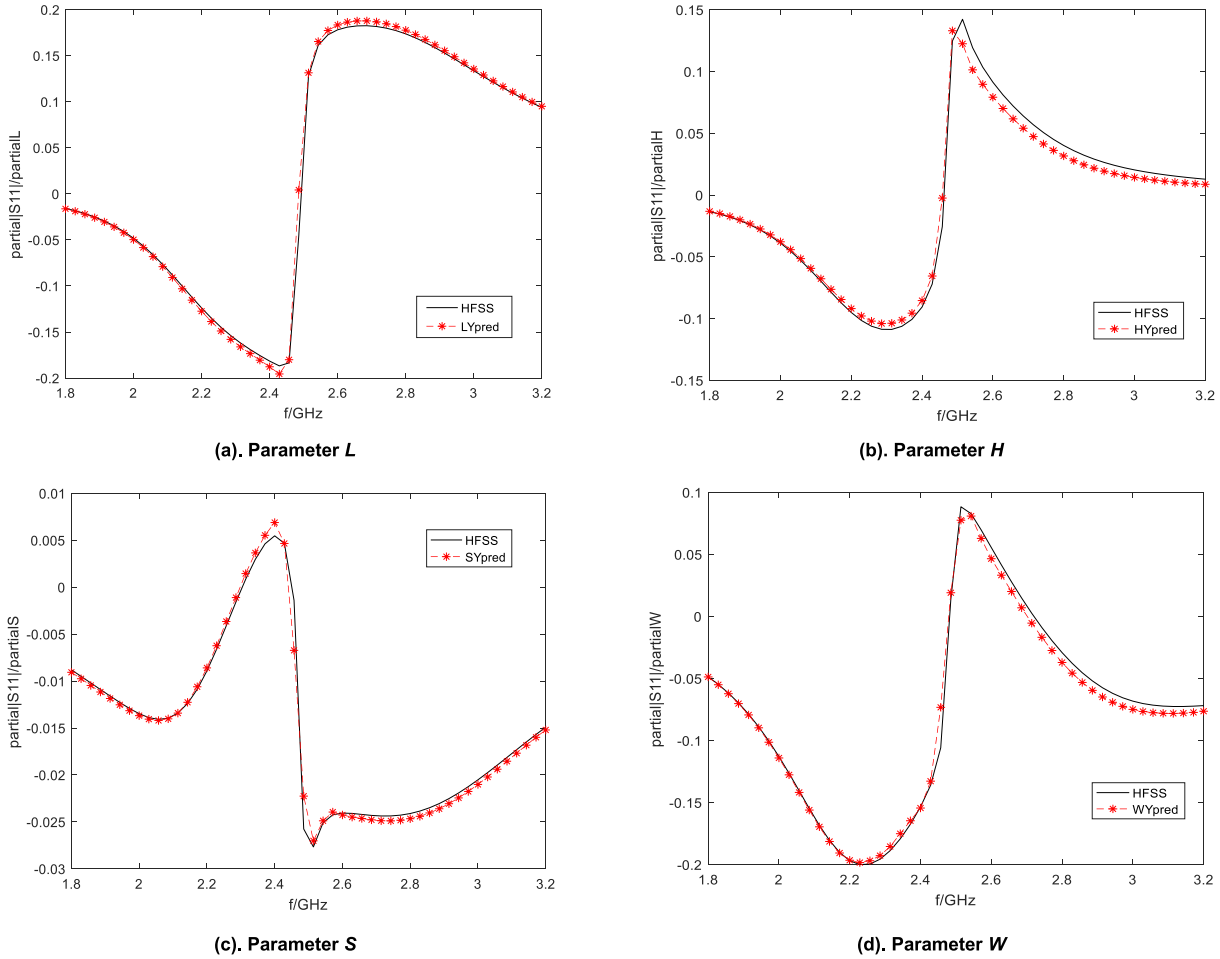

FIGURE 5. Sensitivity simulation results of the optimized inverted F antenna.

TABLE 5. Training and test samples for the ultra-wideband planar monopole antenna.

Parameters (Sensitivity Variables)	Training data			Testing data		
	Min	Max	Step	Min	Max	Step
L_1(mm)	5	6.2	0.2	5.1	6.1	0.2
L_2(mm)	0.4	1	0.1	0.45	0.95	0.1
W_1(mm)	2	3.2	0.2	2.1	3.1	0.2
W_2(mm)	2.4	3.6	0.2	2.5	3.5	0.2
R_1(mm)	5.4	6.6	0.2	5.5	6.5	0.2
R_2(mm)	9	10.2	0.2	9.1	10.1	0.2

optimized prediction results can fit well, accurately reflecting the relationship between the input and output of the antenna performance. Figure 4 is the three-dimensional radiation pattern of the optimized Inverted-F antenna.

Since the sensitivity information of each parameter is considered in the modeling process, the information fitting effect is also good, as shown in Figure 5. The optimized result can also clearly hint the degree of influence of each parameter on the result. Among them, the value of the parameter L has the greatest impact on the antenna performance, and the parameter S has the least impact.

B. THE ULTRA-WIDEBAND PLANAR MONOPOLE ANTENNA

The structure of the ultra-wideband planar monopole antenna in [40] is shown in Figure 6(a), and HFSS model is shown in Figure 6(b), which includes substrate layer, circular ring radiating element, rectangular microstrip feeder, and reference ground for rectangular gaps. The substrate layer is FR4 material with length $L = 42$mm, width $W = 30$mm, thickness $h = 1$mm, relative dielectric constant $\varepsilon_r = 4.4$, and loss tangent $\tan\delta = 0.02$. The radiating unit on the top of the substrate layer is a circular sheet of inner ring R_1, outer

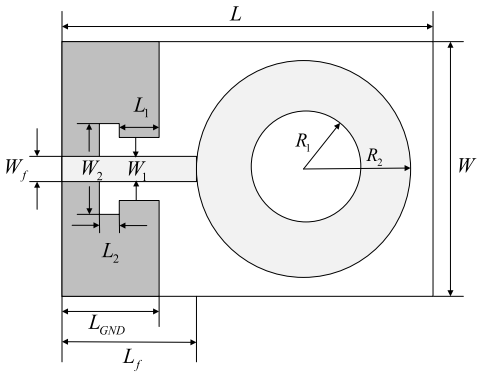

(a). structure diagram

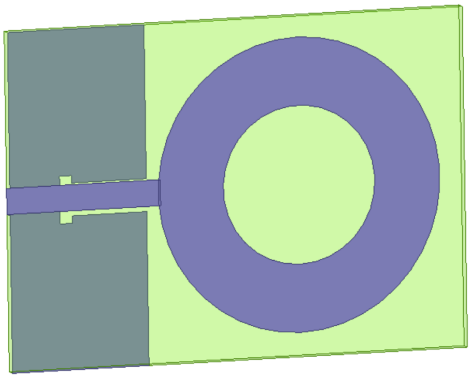

(b). HFSS model

FIGURE 6. The ultra-wideband planar monopole antenna.

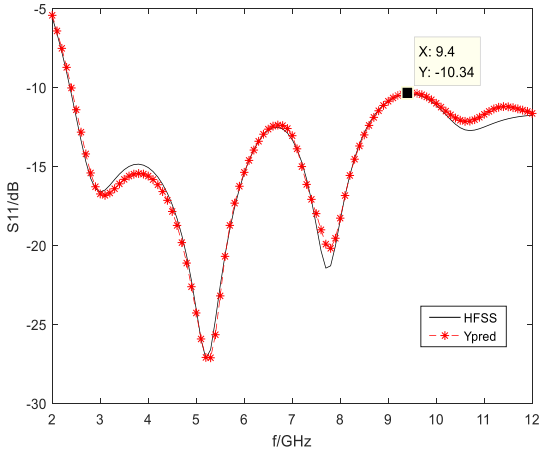

FIGURE 7. S_{11} of the optimized ultra-wideband planar monopole antenna.

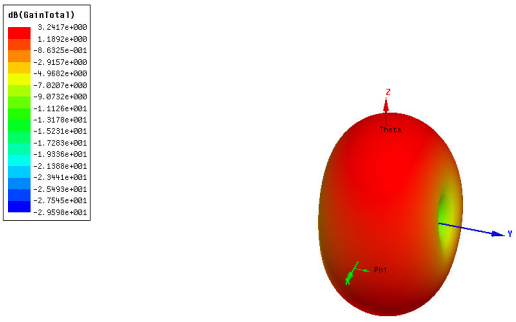

FIGURE 8. Three-dimensional gain pattern of the optimized ultra-wideband planar monopole antenna.

ring R_2, and a rectangular microstrip feeder is with length $L_f = 14.2$mm and width $W_f = 1.96$mm. The bottom is a rectangular structure with a width of $L_{\text{GND}} = 2.6$mm, and two rectangular slits of $L_1 \times W_1$ and $L_2 \times W_2$ are engraved on it. The electromagnetic performance of the antenna is mainly determined by the size of the two rectangular slots and the radius of the inner and outer rings of the circular thin plate. The design ranges are $L_1 = [5,6.2]$mm, $L_2 = [0.4,1]$ mm, $W_1 = [2,3.2]$mm, $W_2 = [2.4,3.6]$mm, $R_1 = [5.4,6.6]$ mm, $R_2 = [9,10.2]$mm. Among them, the upper and lower limit width of the design variables are determined according to the empirical values of [26]. The optimization indexes are that the value of S_{11} in the 3GHz∼11GHz frequency band is less than -10dB.

Similarly, the number of HFSS with coarse grid is 3, fine grid is 7, precision is 0.02, and sensitivity variables are L_1, L_2, W_1, W_2, R_1 and R_2. In the first stage, number of training samples is 50, with 101 frequency points for one sample, and the training input is $\{\boldsymbol{u}_i = [\boldsymbol{X}_i, f_{ih}] = [L_{1i}, L_{2i}, W_{1i}, W_{2i}, R_{1i}, R_{2i}, f_{ih}] | i = 1, 2, \cdots, n\}$. According to the n ($n = 50$) groups of antennas selected in the experiment, we can obtain $\boldsymbol{y}_{\text{coar,perf},i}$ and $\boldsymbol{y}_{\text{coar,sens},i}$, namely $|S_{11}|_{coar}$, and $\frac{d|S_{11}|}{dL_1}_{\text{coar}}$, $\frac{d|S_{11}|}{dL_2}_{\text{coar}}$, $\frac{d|S_{11}|}{dW_1}_{\text{coar}}$, $\frac{d|S_{11}|}{dW_2}_{\text{coar}}$, $\frac{d|S_{11}|}{dR_1}_{\text{coar}}$, $\frac{d|S_{11}|}{dR_2}_{\text{coar}}$ by HFSS with coarse grid to form $\boldsymbol{D}_{\text{coar,perf}}$ an $\boldsymbol{D}_{\text{coar,sens}}$. 20 groups are randomly selected from the 50 groups of samples, and we use HFSS with fine grid to simulate the $\boldsymbol{y}_{\text{fine,perf},i}$ and $\boldsymbol{y}_{\text{fine,sens},i}$, namely $|S_{11}|_{\text{fine}}$, and $\frac{d|S_{11}|}{dL_1}_{\text{fine}}$, $\frac{d|S_{11}|}{dL_2}_{\text{fine}}$, $\frac{d|S_{11}|}{dW_1}_{\text{fine}}$, $\frac{d|S_{11}|}{dW_2}_{\text{fine}}$, $\frac{d|S_{11}|}{dR_1}_{\text{fine}}$, $\frac{d|S_{11}|}{dR_2}_{\text{fine}}$ to form $\boldsymbol{D}_{\text{fine,perf}}$ and $\boldsymbol{D}_{\text{fine,sens}}$. According to the 20 groups of samples given by HFSS with coarse and fine grid, the antenna performance GP_1 and sensitivity GP_3 are established, and then use them to predict the remaining 30 groups of $\boldsymbol{y}_{\text{pred,perf},j}$ and $\boldsymbol{y}_{\text{pred,sens},j}$, namely $|S_{11}|_{pred}$, and $\frac{d|S_{11}|}{dL_1}_{\text{pred}}$, $\frac{d|S_{11}|}{dL_2}_{\text{pred}}$, $\frac{d|S_{11}|}{dW_1}_{\text{pred}}$, $\frac{d|S_{11}|}{dW_2}_{\text{pred}}$, $\frac{d|S_{11}|}{dR_1}_{\text{pred}}$, $\frac{d|S_{11}|}{dR_2}_{\text{pred}}$. Finally, we combine the 20 groups of high-fidelity simulation samples given by HFSS and the 30 groups of predicted 'precise' samples given by the trained GP_1 and GP_3 to form new training samples, namely $\boldsymbol{D}_{\text{fine,perf,appr}}$ and $\boldsymbol{D}_{\text{fine,sens,appr}}$, and then use them to train antenna performance GP_2 and the sensitivity GP_4. The definition of the training sample and test sample of the ultra-wideband planar monopole antenna is shown in Table 5, and the test results of the trained two-stage GP model considering the sensitivity information are shown in Table 6. It can be seen that the MAE is about 0.5 and the RMSE is about 0.7.

Comparing the errors of the above two antenna cases with classical GP and two-stage GP without considering the sensitivity, the result is shown in Table 7. We can conclude that under the same data, because the classical GP

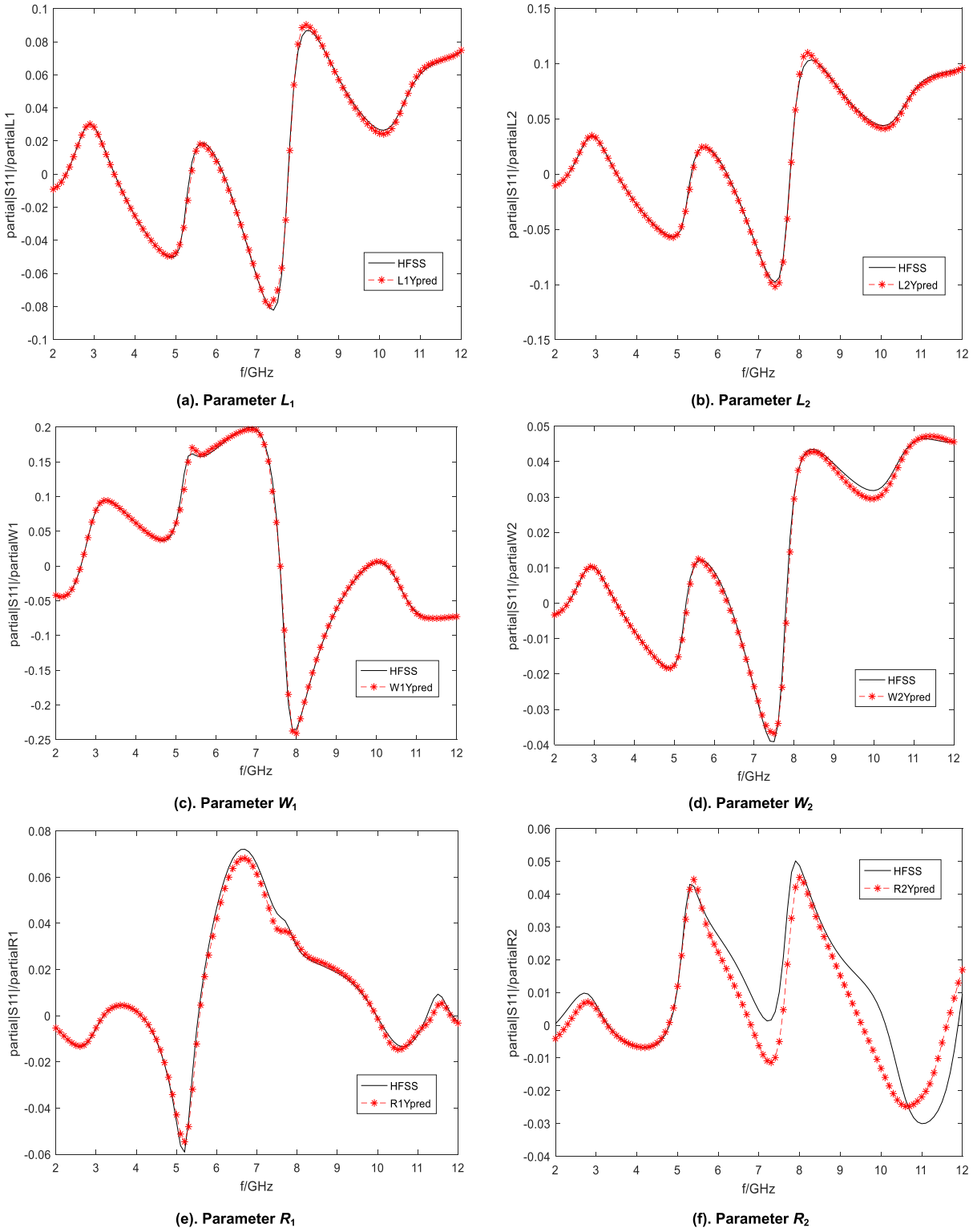

FIGURE 9. Sensitivity simulation results of the optimized ultra-wideband planar monopole antenna.

doesn't have enough training sample and doesn't consider sensitivity information, the test error is relatively large; the test error of the two-stage GP is smaller than that of the classical GP because of more training samples obtained by the two-stage process. In comparison, the proposed two-stage GP considering sensitivity information has smallest test errors and best predicted results.

Taking the trained two-stage GP considering sensitivity information as fitness function, we use PSO to optimize the antenna, and the result is [5.7399 0.7013 2.6614 3.0791

TABLE 6. Errors of different test samples for the ultra-wideband planar monopole antenna.

No.	1	2	3	4	5
MAE(dB)	0.5461	0.4595	0.5693	0.5495	0.4743
RMSE(dB)	0.8025	0.5843	0.6935	0.7074	0.5745

TABLE 7. Comparison of the test samples average error of different model.

Application	GP		Two-stage GP		Two-stage GP considering Sensitivity	
	MAE	RMSE	MAE	RMSE	MAE	RMSE
Case 1	1.0634	1.8561	0.5835	0.9867	0.4666	0.6620
Case 2	1.2672	2.0933	0.6979	1.0754	0.5197	0.6724

5.9604 9.7004] mm, and its S_{11} is shown in Figure 7, where the black solid represents the simulation result by electromagnetic simulation software HFSS, and the red dash line with star represents the predicted result by the proposed algorithm. It can be seen from Figure 7 that the value of $|S_{11}|$ in the frequency range of 3GHz $\sim$ 11GHz is less than -10dB, which can completely cover the 3.1GHz $\sim$ 10.6GHz band assigned by the Federal Communications Commission for UWB services, which meets the design requirements. And the prediction result of the surrogate model can fit the simulation of electromagnetic simulation software well. Figure 8 shows the three-dimensional radiation pattern of the optimized UWB planar monopole antenna at 5GHz with 3.24dB gain. Similarly, considering the sensitivity information relative to each parameter, as shown in Figure 9, it can be seen that the fitting effect is relatively excellent, and the value of parameter W_1 has the greatest influence on the performance of the antenna, and parameter W_2 has the least influence. This example again verifies the effectiveness of the proposed method.

IV. CONCLUSION

In order to reduce the computational cost of obtaining training samples by high-fidelity full-wave electromagnetic simulation software and enhance the efficiency of antenna optimization design, this paper develops a two-stage Gaussian process considering sensitivity information model. The training samples of the second stage come from the high-fidelity response data obtained by the full-wave electromagnetic simulation software with fine grid and 'precise' predicted data by the first stage GP model trained by coarse grid data. Since the simulation time of electromagnetic simulation software with coarse grid is much shorter than that of with fine grid, it can greatly save time. While establishing the two-stage Gaussian process, the sensitivity information is also considered. Without the need for a large number of training samples, the change trend of the electromagnetic response can also be obtained, and an accurate surrogate model can be established. Therefore, in the problem of insufficient samples or high sample acquisition costs, the consideration of sensitivity information is particularly important for improving the trained model's performance. In addition, the surrogate model can not only obtain better antenna performance response, but also sensitivity information of different geometric parameters. It is convenient for developers to follow-up development. Finally, the method is evaluated through the modeling and optimization of the inverted F antennas and the ultra-wideband planar monopole antennas with a small amount of sample data. The experimental results show that a more accurate surrogate model can be obtained even in the case of few high-fidelity training samples, which further verifies the effectiveness and efficiency of the proposed modeling method.

However, the method proposed in this paper is of little significance to big data problems, because if we have enough training sample, we don't need to perform the first stage GP. Simultaneously, the efficiency is low for big data because the computing burden is the cube of number of the training samples. But, we all know most design and optimization missions in the electromagnetic field domain belong to small samples, which can apply the proposed approach very well.

ACKNOWLEDGMENT

(Rui Li and Yubo Tian are co-first authors.)

REFERENCES

[1] M. B. Steer, J. W. Bandler, and C. M. Snowden, "Computer-aided design of RF and microwave circuits and systems," *IEEE Trans. Microw. Theory Techn.*, vol. 50, no. 3, pp. 996–1005, Mar. 2002.

[2] A. Lalbakhsh, M. U. Afzal, and K. Esselle, "Simulation-driven particle swarm optimization of spatial phase shifters," in *Proc. Int. Conf. Electromagn. Adv. Appl. (ICEAA)*, Cairns, QLD, Australia, Sep. 2016, pp. 428–430.

[3] A. Lalbakhsh, M. U. Afzal, K. P. Esselle, and S. Smith, "Design of an artificial magnetic conductor surface using an evolutionary algorithm," in *Proc. Int. Conf. Electromagn. Adv. Appl. (ICEAA)*, Verona, Italy, Sep. 2017, pp. 885–887.

[4] Y.-L. Li, W. Shao, L. You, and B.-Z. Wang, "An improved PSO algorithm and its application to UWB antenna design," *IEEE Antennas Wireless Propag. Lett.*, vol. 12, pp. 1236–1239, 2013.

[5] S. Rani and A. P. Singh, "On the design and optimisation of new fractal antenna using PSO," *Int. J. Electron.*, vol. 100, no. 10, pp. 1383–1397, Oct. 2013.

[6] L. Wakrim, S. Ibnyaich, and M. M. Hassani, "The study of the ground plane effect on a multiband PIFA antenna by using genetic algorithm and particle swarm optimization," *J. Microw., Optoelectron. Electromagn. Appl.*, vol. 15, no. 4, pp. 293–308, Dec. 2016.

[7] M. Ding, R. Jin, and J. Geng, "Optimal design of ultra wideband antennas using a mixed model of 2-D genetic algorithm and finite-difference time-domain," *Microw. Opt. Technol. Lett.*, vol. 49, no. 12, pp. 3177–3180, 2007.

[8] B. Tian, Z. Li, and C. Wang, "Boresight gain optimization of an UWB monopole antenna using FDTD and genetic algorithm," in *Proc. IEEE Int. Conf. Ultra-Wideband*, Nanjing, China, Sep. 2010, pp. 1–4.

[9] P. Lalbakhsh, B. Zaeri, and A. Lalbakhsh, "An improved model of ant colony optimization using a novel pheromone update strategy," *IEICE Trans. Inf. Syst.*, vol. E96.D, no. 11, pp. 2309–2318, 2013.

[10] L. Chang, C. Liao, W. Lin, L.-L. Chen, and X. Zheng, "A hybrid method based on differential evolution and continuous ant colony optimization and its application on wideband antenna design," *Prog. Electromagn. Res.*, vol. 122, pp. 105–118, 2012.
[11] S. Adibi, M. A. Honarvar, and A. Lalbakhsh, "Gain enhancement of wide-band circularly polarized UWB antenna using FSS," *Radio Sci.*, vol. 56, no. 1, Jan. 2021.
[12] S. Koziel and S. Ogurtsov, "Multilevel microwave design optimization with automated model fidelity adjustment," *Int. J. RF Microw. Comput.-Aided Eng.*, vol. 24, no. 3, pp. 281–288, May 2014.
[13] J. W. Bandler, J. E. Rayas-Sanchez, and Q. J. Zhang, "Yield-driven EM optimization using space mapping-based neuromodels," in *Proc. 31st Eur. Microw. Conf.*, London, U.K., Oct. 2001, pp. 1–4.
[14] A. Pietrenko-Dabrowska, S. Koziel, and M. Al-Hasan, "Expedited yield optimization of narrow- and multi-band antennas using performance-driven surrogates," *IEEE Access*, vol. 8, pp. 143104–143113, 2020.
[15] L.-Y. Xiao, W. Shao, F.-L. Jin, and B.-Z. Wang, "Multiparameter modeling with ANN for antenna design," *IEEE Trans. Antennas Propag.*, vol. 66, no. 7, pp. 3718–3723, Jul. 2018.
[16] L. H. Manh, F. Grimaccia, M. Mussetta, and R. E. Zich, "Optimization of a dual ring antenna by means of artificial neural network," *Prog. Electromagn. Res. B*, vol. 58, pp. 59–69, 2014.
[17] Y. Chen, Y. Tian, and M. Le, "Modeling and optimization of microwave filter by ADS-based KBNN," *Int. J. RF Microw. Comput.-Aided Eng.*, vol. 27, no. 2, Feb. 2017, Art. no. e21062.
[18] F. Sun, Y. Tian, G. Hu, and Q. Shen, "DOA estimation based on support vector machine ensemble," *Int. J. Numer. Model., Electron. Netw., Devices Fields*, vol. 32, no. 5, p. e2614, May 2019.
[19] T. Khan and C. Roy, "Prediction of slot-position and slot-size of a microstrip antenna using support vector regression," *Int. J. RF Microw. Comput.-Aided Eng.*, vol. 29, no. 3, Mar. 2019, Art. no. e21623.
[20] S. Fei-Yan, T. Yu-Bo, and R. Zuo-Lin, "Modeling the resonant frequency of compact microstrip antenna by the PSO-based SVM with the hybrid kernel function," *Int. J. Numer. Model., Electron. Netw., Devices Fields*, vol. 29, no. 6, pp. 1129–1139, Nov. 2016.
[21] X. Chen, Y. Tian, T. Zhang, and J. Gao, "Differential evolution based manifold Gaussian process machine learning for microwave Filter's parameter extraction," *IEEE Access*, vol. 8, pp. 146450–146462, 2020.
[22] J. Gao, Y. Tian, and X. Chen, "Modeling of antenna resonant frequency based on co-training of semi-supervised Gaussian process with different kernel functions," *Int. J. RF Microw. Comput.-Aided Eng.*, vol. 31, no. 6, Jun. 2021.
[23] J. Gao, Y. Tian, and X. Chen, "Antenna optimization based on co-training algorithm of Gaussian process and support vector machine," *IEEE Access*, vol. 8, pp. 211380–211390, 2020.
[24] C. E. Rasmussen, "Gaussian processes in machine learning," in *Proc. Summer School Mach. Learn.* Berlin, Germany: Springer, 2004, pp. 63–71.
[25] Y.-X. Xu and Y.-B. Tian, "Optimal design of conical horn antenna based on GP model with coarse mesh," *Iranian J. Sci. Technol., Trans. Electr. Eng.*, vol. 43, no. 4, pp. 717–724, Dec. 2019.
[26] Y. Chen, Y. Tian, Z. Qiang, and L. Xu, "Optimisation of reflection coefficient of microstrip antennas based on KBNN exploiting GPR model," *IET Microw., Antennas Propag.*, vol. 12, no. 4, pp. 602–606, Mar. 2018.
[27] J. Gao, Y. Tian, X. Zheng, and X. Chen, "Resonant frequency modeling of microwave antennas using Gaussian process based on semisupervised learning," *Complexity*, vol. 2020, pp. 1–12, May 2020.
[28] J. P. Jacobs, "Efficient resonant frequency modeling for dual-band microstrip antennas by Gaussian process regression," *IEEE Antennas Wireless Propag. Lett.*, vol. 14, pp. 337–341, 2015.
[29] X.-Y. Zhang, Y.-B. Tian, and X. Zheng, "Antenna optimization design based on deep Gaussian process model," *Int. J. Antennas Propag.*, vol. 2020, pp. 1–10, Nov. 2020.
[30] S. A. Sadrossadat, Y. Cao, and Q.-J. Zhang, "Parametric modeling of microwave passive components using sensitivity-analysis-based adjoint neural-network technique," *IEEE Trans. Microw. Theory Techn.*, vol. 61, no. 5, pp. 1733–1747, May 2013.
[31] F. Feng, V.-M.-R. Gongal-Reddy, C. Zhang, J. Ma, and Q.-J. Zhang, "Parametric modeling of microwave components using adjoint neural networks and pole-residue transfer functions with EM sensitivity analysis," *IEEE Trans. Microw. Theory Techn.*, vol. 65, no. 6, pp. 1955–1975, Jun. 2017.
[32] F. Feng, W. Na, W. Liu, S. Yan, L. Zhu, and Q.-J. Zhang, "Parallel gradient-based EM optimization for microwave components using Adjoint- sensitivity-based neuro-transfer function surrogate," *IEEE Trans. Microw. Theory Techn.*, vol. 68, no. 9, pp. 3606–3620, Sep. 2020.
[33] J. Zhang, F. Feng, W. Zhang, J. Jin, J. Ma, and Q.-J. Zhang, "A novel training approach for parametric modeling of microwave passive components using Padé via lanczos and EM sensitivities," *IEEE Trans. Microw. Theory Techn.*, vol. 68, no. 6, pp. 2215–2233, Jun. 2020.
[34] K.-C. Lee, "Application of neural network and its extension of derivative to scattering from a nonlinearly loaded antenna," *IEEE Trans. Antennas Propag.*, vol. 55, no. 3, pp. 990–993, Mar. 2007.
[35] Q. S. Cheng, J. W. Bandler, and N. K. Nikolova, "Fast space mapping modeling with adjoint sensitivity," in *IEEE MTT-S Int. Microw. Symp. Dig.*, Baltimore, MD, USA, Jun. 2011, pp. 1–4.
[36] J. P. Jacobs and S. Koziel, "Two-stage framework for efficient Gaussian process modeling of antenna input characteristics," *IEEE Trans. Antennas Propag.*, vol. 62, no. 2, pp. 706–713, Feb. 2014.
[37] R. B. Gramacy and H. K. H. Lee, "Bayesian treed Gaussian process models with an application to computer modeling," *J. Amer. Stat. Assoc.*, vol. 103, no. 483, pp. 1119–1130, Sep. 2008.
[38] Y. X. Xu, Y. B. Tian, and X. P. Hu, "Design of dual-frequency microstrip antenna based on Gaussian process of a new kernel function," *Comput. Appl. Res.*, vol. 35, no. 8, pp. 2477–2479, 2483, 2018.
[39] Y.-X. Xu, Y.-B. Tian, and X.-P. Hu, "Antenna modeling method based on two-stage Gaussian process," *Appl. Res. Comput.*, vol. 35, no. 10, pp. 3062–3064, 2018.
[40] S.-Y. Sun, Y.-H. Lv, and J.-L. Zhang, "Design and optimization of UWB antenna based on genetic algorithm," *Chin. J. Radio Sci.*, vol. 1, pp. 62–66, Oct. 2011.

RUI LI was born in Yancheng, China, in 1996. She is currently pursuing the degree with the Jiangsu University of Science and Technology. Her research interest includes signal processing theory and technology.

YUBO TIAN was born in Tieling, Liaoning, China, in 1971. He received the Ph.D. degree in radio physics from the Department of Electronic Science and Engineering, Nanjing University, Nanjing, China. From 1997 to 2004, he was with the Department of Information Engineering, Shenyang University, Shenyang, China. He was a Visiting Scholar with the University of California at Los Angeles, in 2009, and Griffith University, in 2015. From 2005 to 2020, he was with the School of Electronics and Information, Jiangsu University of Science and Technology, Zhenjiang, China, where he has been a Full Professor and the Vice Dean, since 2011. He is currently with the School of Information and Communication Engineering, Guangzhou Maritime University, Guangzhou, China. He has authored or coauthored more than 100 journal articles and three books. He also holds more than 20 filed/granted China patents. His current research interest includes machine learning methods and their applications in electronics and electromagnetics.

PENGFEI LI was born in Taizhou, China, in 1994. He received the bachelor's degree from the Jiangsu University of Science and Technology, in 2018, where he is currently pursuing the master's degree. His research interests include deep learning and array signal processing.